Journal of Photochemistry and Photobiology 25 (2025) 100258

Contents lists available at ScienceDirect

Journal of Photochemistry and Photobiology

journal homepage: www.sciencedirect.com/journal/journal-of-photochemistry-and-photobiology

Nonthermal atmospheric pressure plasma (NTAPP) effectively eliminates skin tumors in a mouse model of UV-induced carcinogenesis with a short-term treatment regimen

Szabolcs Bozsányi [a,b], Ruby Acquah [a,b], Rhea Carmel Glen Rodrigues [a,b], Erin C. Tracy [a,b], Sean P. Murphy [a,b], Gregory Fridman [c], Wendy J. Huss [a,b], Peter C. Friedman [d,*], Gyorgy Paragh [a,b,*]

[a] Department of Dermatology, Roswell Park Comprehensive Cancer Center, Buffalo, NY, 14263, USA
[b] Department of Cell Stress Biology, Roswell Park Comprehensive Cancer Center, Buffalo, NY, 14263, USA
[c] AAPlasma LLC, Philadelphia, PA, 19146, USA
[d] The Skin Center Dermatology Group, New City, NY, 10956, USA

ARTICLE INFO

Keywords:
Nonthermal atmospheric pressure plasma
NTAPP
UV
Skin cancer
Early topical treatment

ABSTRACT

Introduction: Nonthermal atmospheric pressure plasma (NTAPP) therapy has emerged as a promising modality in dermatology for wound healing, tissue regeneration, and anti-tumor applications. This study evaluated the feasibility and effectiveness of a simple, one-week NTAPP treatment protocol in the SKH1 hairless mouse model of chronic ultraviolet (UV) radiation-induced carcinogenesis.

Materials and methods: SKH1 mice were exposed to solar-simulated UV light 5 times a week for 10 weeks, which produced multiple skin tumors on each mouse. At week 25 NTAPP treatment was administered to a subgroup of mice at a setting of 20 kV with a 20 ns pulse width and 200 Hz frequency three times within a single week. A total of 31 NTAPP-treated and 34 internal control tumors (i.e., nearby tumors on the same mouse) in UV-exposed, NTAPP-treated mice were evaluated for tumor size at 0 and 28 days after the beginning of the treatment by using ImageJ on standardized photographs. A subset of the tumors was also assessed with a 33 MHz high-frequency ultrasound (HFUS) to measure vertical tumor thickness. In similarly housed control mice, sizes of 64 tumors were evaluated as external controls.

Results: NTAPP induced a significant reduction in the mean tumor area from 5.65 ± 6.51 mm^2 before treatment to 1.74 ± 3.99 mm^2 28 days post-treatment (paired *t*-test, $p = 0.0016$). Internal control tumors, in contrast, showed an increase in area from 3.24 ± 2.54 mm^2 before treatment to 4.57 ± 3.58 mm^2 28 days post-treatment (paired *t*-test, $p = 0.0296$). Of the 31 treated tumors, 23 completely disappeared; in contrast, only six non-treated internal control tumors disappeared ($p = 0.0139$, two-sided chi-square test). Simultaneously, optically guided HFUS revealed a significant decrease in tumor thickness in treated areas (paired *t*-test, $p = 0.0006$), with no significant changes observed in the internal control tumors (paired *t*-test, $p = 0.5555$). External control tumors showed an increase in size, which was not statistically significant.

Discussion: The results demonstrated that a one-week NTAPP protocol could effectively eliminate 74 % of mouse tumors induced by UV radiation. These findings warrant further investigations of short, clinically feasible NTAPP treatment protocols for early skin cancer treatment.

1. Introduction

Ultraviolet (UV) radiation is one of the best characterized environmental carcinogens [1]. Chronic UV exposure, cumulative solar UV radiation, and the number of sunburns are associated with melanoma and non-melanoma skin cancer (NMSC) risk [2,3]. NMSCs are the most common human cancers and have shown a continued rise in incidence in recent decades [4]. NMSCs originate within the epidermal layer [5], and they consist of two main subtypes: basal cell carcinoma (BCC), which is responsible for two-thirds of all NMSC cases, and cutaneous squamous

* Corresponding authors.
E-mail addresses: pbc9@cumc.columbia.edu (P.C. Friedman), gyorgy.paragh@roswellpark.org (G. Paragh).

https://doi.org/10.1016/j.jpap.2024.100258

Available online 2 January 2025
2666-4690/© 2024 Published by Elsevier B.V. This is an open access article under the CC BY-NC-ND license (http://creativecommons.org/licenses/by-nc-nd/4.0/).

cell carcinoma (cSCC), responsible for one-third of NMSC cases [4]. Currently, the gold standard treatment for cSCC is surgical removal [6], but non-surgical treatment options would be helpful in early neo-adjuvant settings, for combinatorial treatments, or when surgery is not possible. Here, we evaluate the effectiveness of a simple, one-week nonthermal atmospheric pressure plasma (NTAPP) treatment protocol in an SKH1 hairless mouse model of UV radiation-induced carcinogenesis. SKH1 hairless mice are the most widely used preclinical model of UV-related carcinogenesis [7–9]. After chronic irradiation, many skin tumors appear on the mouse skin, with histological features of actinic keratoses, keratoacanthomas, in situ SCCs, and invasive cSCCs [10].

Plasma, in general, is a partially or completely ionized gaseous state of matter [11], which can be classified into different subcategories based on gas pressure (low- vs. atmospheric pressure) or based on temperature (hot/thermal vs. cold/nonthermal) [12]. Nonthermal atmospheric pressure plasma (NTAPP), or as it is also called, cold atmospheric plasma, is a promising tool in dermatology [13], using plasma constituents like reactive oxygen and nitrogen species, UV photons, and electromagnetic emissions [14]. Unlike traditional thermal plasmas, NTAPP operates at lower temperatures and is thus well-suited for medical and cosmetic procedures [12,15]. Moreover, the noninvasive nature of NTAPP makes it an attractive option for dermatological treatments, as this minimizes patient discomfort by reducing pain and recovery times [16]. NTAPP has demonstrated efficacy in various settings, including for stimulating wound healing [15] and hair follicles [17], promoting tissue regeneration [18], and activating adult stem cells [19,20]. The controlled generation of reactive oxygen and nitrogen species by NTAPP also has antimicrobial properties, offering a novel approach to combatting infections [21]. Additionally, NTAPP has shown potential in promoting collagen synthesis and improving wound healing and blood circulation, contributing to enhanced skin rejuvenation and scar reduction [15,22,23].

In oncology, NTAPP has shown efficacy in several treatment applications including the field of dermato-oncology. NTAPP's anti-tumor properties mostly rely on the induction of cell cycle arrest [24], ultimately leading to apoptosis of the malignant proliferative cells [12,25,26]. Cold atmospheric plasma is known to upregulate tissue catalase in both UV-exposed and non-UV-exposed skin and decreases the pathological proliferation of UVB-induced skin lesions. Cold atmospheric plasma has proven to be effective in treating head and neck carcinomas [27,28], actinic keratoses [11,29], squamous cell carcinoma [23], and melanoma in mice [30]. The relative selectivity of plasma for killing tumor cells can be explained by the increased metabolic activity of tumor cells with concomitantly high ROS and RNA levels, which makes tumor tissue more susceptible to plasma-induced oxidative stress [31]. Moreover, plasma tends to affect cells during DNA replication, which also increases the effects of plasma on tumor cells [32].

Although NTAPP has shown promise in skin cancer treatment, knowledge of the current clinical utility of NTAPP for this purpose is limited. Easy-to-adopt and clinically feasible protocols for using NTAPP in the skin treatment setting do not exist, and to date, the efficacy of short-term NTAPP treatments on skin tumors has not been established. To fill this critical gap and provide crucial preliminary data for future studies, we show here in the SKH1 model of chronic UV carcinogenesis that NTAPP effectively eliminates a high percentage of skin tumors in a short one-week, well-tolerated treatment regimen.

2. Materials and methods

2.1. UV-induced carcinogenesis in SKH1 mice

All animal procedures were conducted in accordance with the guidelines and based on an Institutional Animal Care and Use Committee (IACUC) approved protocol at Roswell Park Comprehensive Cancer Center. Roswell Park has an AAALAC International Accredited Animal Program. SKH1 mice for the breeding colony (strain name: SKH1-hrhr) [7] were purchased from Charles River Laboratories (Wilmington, MA) and outbred progeny were used for these studies. SKH1 mice were housed in a controlled environment with a 12-hour light/dark cycle and provided with standard rodent chow and water ad libitum. Six SKH1 mice (three females and three males) were irradiated with 90 mJ/cm^2, this was the energy of the UVB radiation (the output was controlled by using power meter and the measured ratio of UVB/UVA was 4.8 %) five days a week with the Abet 11044–1 Solar Simulator for 10 weeks, starting at 6–8 weeks of age plus seven external control SKH1 mice were also followed, altogether 13 mice were irradiated and six of them has a subset of tumors plasma treated. The Abet 11044–1 Solar Simulator (source) includes a 11063 Atmospheric Edge Filter and delivers light with a terrestrial match from 290 nm to 400 nm over an illumination field of 200 mm × 200 mm in a broad spectrum, encompassing both UVA and UVB light in a spectral distribution similar to the terrestrial UV irradiance. The edge filter eliminates UVC and prevents significant heating of the mice during treatment. Mice were followed, and tumors were treated with NTAPP during experimental week 25, 15 weeks after UV irradiation ended. Two tattoo dots were also used to help localize skin lesions and track the tumors. During the NTAPP treatment, the animals were anesthetized with ketamine. The mice were under anesthesia during treatment to reduce the stress the animals would have experienced during the prolonged immobilization period and to facilitate accurate plasma delivery [23]; the plasma treatment itself is not painful [33,34].

2.2. Plasma treatment and mice data

A pulse generator (FPG10–01NM10, FID GmbH, Burbach, Germany) was employed to generate plasma. The generator supplied a 20-kV pulse with a pulse width of 20 ns at a frequency of 200 Hz. The plasma was created by applying these parameters to a 5-mm diameter quartz-covered copper electrode. The electrode is 10 cm long, and the quartz thickness is 1 mm.

The UV-exposed mice each had multiple lesions, 5–6 large lesions were treated with generated plasma on the upper part of the back, and 5–6 lesions of similar or smaller size were selected as internal control tumors on each mouse on the bottom part of the back. There were a total of 31 NTAPP-treated (abbreviated as plasma-treated or treated) tumors and 34 non-treated internal control tumors. Each lesion was treated three times for 2 min on three days within a seven-day period (treated on 3 non-consecutive days over a 7-day period) and was followed for 28 days.

A non-NTAPP-treated cohort of similar solar simulator-treated mice ($n = 7$) was also followed for 28 days to establish the growth kinetics of tumors in the same model in non-plasma-treated mice at the same phase of chronic UV carcinogenesis (external controls). Their size-matched tumors served as absolute control for the plasma treatment. This was done to exclude the potential systemic effects of the abscopal-like effect of plasma treatment or systemic effects similar to the ones described in topical field treatments [35,36]. All the treated tumors and internal controls ($n = 65$ tumors) were size-matched with the external controls ($n = 65$ tumors).

2.3. Photographic and dermoscopic imaging

The mice were photographed weekly from 3 different angles with a fixed digital single-lens reflex (DSLR) camera setup under standard lighting conditions to follow the treatment response. Dermoscopy (epiluminescence microscopy [37]) and photographic images of the lesions were captured before and after each treatment session, and the mice were photographed weekly for 28 days following treatment to monitor for any changes in size, appearance, or other relevant characteristics as an effect of the plasma treatment. Each tumor was measured in the photographic images to calculate the tumor area, and the number of pixels in each area was determined with ImageJ software [38]. For

questionable lesions, dermoscopic photos and photos from different camera angles were compared to each other. Additionally, two investigators anonimous to the study validated the tumor annotations (R. A., R.C.G.R.).

2.4. High-frequency ultrasound (HFUS) imaging

Optically guided high-frequency ultrasound (OG-HFUS) imaging with a portable OG-HFUS device was performed on a subset of three mice to examine the treatment effects on the lesions (Dermus Skin-Scanner, Dermus Ltd., Budapest, Hungary). The OG image helped direct the HFUS imaging on the skin to measure thickness, similar to our previous experiments on tumor thickness and OG-HFUS features in melanoma [39] and BCC [40]. HFUS imaging was performed on treated and internal control tumors immediately before the plasma treatment and 28 days post-treatment. A minimum of five cross-sectional images were captured for each lesion to conduct a comprehensive assessment. The OG-HFUS device was used to capture optical images with a single-element ultrasound transducer featuring a nominal center frequency of 33 MHz. The resultant ultrasound image was presented using a color scale to enhance contrast. The optical image provided a field of view measuring 15 mm × 15 mm, while the ultrasound image extended 12 mm laterally and achieved a maximum penetration depth of 10 mm.

2.5. Statistical analysis methods, area, and tumor depth measurements

Paired *t*-tests were used to compare the tumor area and thickness before and after treatments. Chi-square tests were used to compare the number of visible tumors before and 28 days after the beginning of the treatments. Two-way ANOVAs were used to compare the sex-related differences between tumor sizes in male and female mice. Statistical tests were performed using GraphPad Prism v8.0.1. software (GraphPad Software Inc., La Jolla, CA, USA). Tumors and sites of prior tumors were identified based on the location of the previous week, the distance from the tattoos, and the relative position of other tumors. For evaluating change, 150 % percent of the original area/depth or greater were considered growth, 50 % of the original area/depth or smaller was considered shrinkage, while 50–150 % area or depth difference was considered stable. A tumor was classified as having disappeared when these three following criteria were met:

1. Complete Resolution: The tumor and any associated elevation were completely undetectable, leaving no visible trace of the original tumor.
2. Scar or Healthy Tissue Formation: The area previously occupied by the tumor shows either a scar or a change in pigmentation, indicating healing, or the surface of this area appears healthy, and the borders of the former tumor cannot be discerned, suggesting that the underlying tissue has undergone complete remodelling.
3. No Regrowth: During the follow-up period, there has been no evidence of the tumor re-emerging in the same location.

These criteria aim to provide a comprehensive and observable set of conditions to confirm tumor disappearance, encompassing the physical removal of the tumor and the healing and recovery of the affected tissue.

3. Results

3.1. Plasma treatment eliminated the majority of tumors efficiently

We measured the size of the NTAPP-treated and internal control tumors to assess the effects of a short 1-week NTAPP treatment protocol on SKH1 skin tumors. Tumors ($n = 31$) from six mice were treated with plasma, and similar size or smaller tumors ($n = 34$) on the same mice, which were not significantly different from the treated group in size (unpaired *t*-test, $p = 0.0509$, 95 % CI: −4.812 to 0.009874) served as internal control tumors that did not receive plasma treatment. The tumor areas were also assessed in mice ($n = 7$) that did not receive plasma treatment to have controls without the potential for systematic plasma effect or abscopal effect. The tumors ($n = 65$) from these served as external controls and were size-matched to the treated and untreated tumors from mice that received plasma treatment.

There was a significant and, on average, a 69.2 % decrease in the tumor area in the NTAPP-treated tumor cohort compared to their area before treatment. The mean area of the treated tumors was 5.65 ± 6.51 mm^2 before treatment and 1.74 ± 3.99 mm^2 after 28 days (paired t-test, $p = 0.0016$, 95 % CI: −6.21 to −1.61), (Fig. 1A and 1C). The mean tumor area of the internal control tumors increased 41.0 %. The mean internal control tumor area was 3.24 ± 2.55 mm^2 before the treatment timepoint and 4.57 ± 3.58 mm^2 after 28 days (paired *t*-test, $p = 0.0164$, 95 % CI: 0.26 to 2.38). After treatment, 23/31 (74.19 %) of NTAPP-treated tumors disappeared, whereas 6/34 (17.64 %) of the non-NTAPP treated tumors disappeared ($p = 0.0118$, two-sided chi-square probe) (Fig. 1B, 1D and 1E).

To assess tumor sizes in male and female mice following NTAPP treatment, a two-way ANOVA was conducted to evaluate the effects of sex, treatment, and their interaction. The analysis revealed no significant differences in tumor sizes based on sex alone ($F(15, 30) = 1.094$, $p = 0.4013$). There was no significant difference in either of the internal control groups in tumor size in male and female mice ($F(23, 10) = 0.5418$, $p = 0.8916$).

The tumors from the external controls matching the NTAPP-treated tumors showed an average 31.8 % increase in size within the 28-day timepoint. The mean tumor area was 6.72± 6.79 mm^2 at the time of treatment and 8.86 ± 8.95 mm^2 after 28 days, but this increase did not reach statistical significance (paired t-test, $p = 0.0823$, 95 % confidence interval: −0.29 to 4.58; tumor disappearance rate of 2/31 [6.45 %]) (Fig. 1F). The external controls matched to the internal control tumors showed an average 69.7 % increase in size. The mean tumor area was 2.85 ± 1.844 mm^2 at the time of treatments and 4.83 ± 6.202 mm^2 after 28 days, but this increase failed to reach statistical significance (paired t-test, $p = 0.0608$, 95 % confidence interval: −0.09545 to 4.065). The internal controls had a disappearance rate of 6/34 (17.64 %).

3.2. Optically guided high-frequency ultrasound imaging could measure decrease in tumor thickness

We measured a subset of 13 treated tumors and 10 control tumors in 3 mice using HFUS before and 28 days after treatment. The treated and the internal control tumor depths did not differ from each other significantly before treatment (unpaired *t*-test, $p = 0.1005$, CI: −1.074 to 0.1036). Of the 13 treated tumors, 12 disappeared, and the remaining tumors shrank in thickness drastically (from 2.37 mm to 0.64 mm) (Fig. 2A). The mean thickness of the treated areas was 0.862 ± 0.73 mm before the treatment and significantly decreased to 0.044 ± 0.15 mm 28 days after the start of the treatment (paired t-test, $p = 0.0006$, 95 % confidence interval: −1.12 to −0.43). Of the ten control tumors, two disappeared completely with time, four were stable, and four increased in thickness. The mean thickness was 0.47 ± 0.18 mm before the treatments and became 0.53 ± 0.36 mm 28 days post-treatment (Fig. 2A) (paired t-test, $p = 0.55$, 95 % confidence interval: −0.18 to 0.31).

4. Discussion

While there are a few publications on the efficacy of superficial NTAPP in treating actinic keratoses and skin cancers [11,26,29,41], prior treatment protocols are long, making widespread clinical adaptation unlikely [23]. Thus, our current work explored the utility of a short, easily clinically adaptable NTAPP treatment protocol. We assessed the effectiveness of NTAPP in treating chronic photocarcinogenesis-induced skin tumors in the SKH1 hairless mouse model, with only three NTAPP

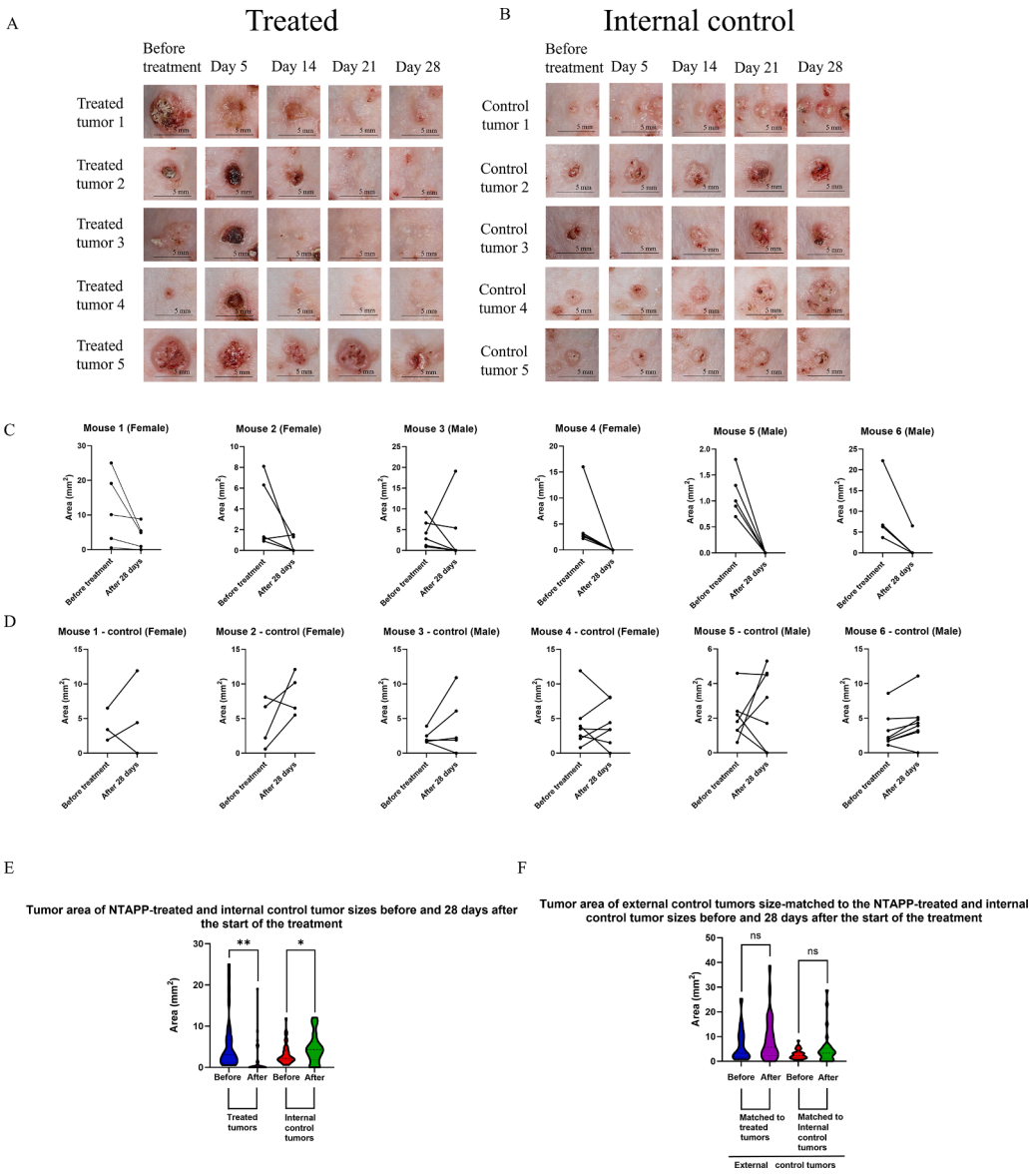


Fig. 1. Effects of NTAPP on Tumor Area Over Time. A, B: Digital photographs of five representative NTAPP-treated (A) and five non-treated internal control tumors (B) in UV-exposed mice during the treatment and follow-up period, 28 days after the beginning of the treatment (images depict 7 mm × 7 mm skin area). Treated tumor 1: shrunk; treated tumor 2: disappeared; treated tumor 3: disappeared; treated tumor 4: disappeared; treated tumor 5: disappeared. Control tumor 1: grew; control tumor 2: stable; control tumor 3: grew; control tumor 4: grew; control tumor 5: stable. C: The NTAPP-treated (C) and non-treated (D) tumor sizes in all six solar simulator-treated mice in the growth kinetics cohort before and after treatment. Each line in every graph stands for a tumor. E: Tumor area measurements in all treated ($n = 31$) and untreated internal control tumors ($n = 34$) in all six UV-exposed mice (**$p = 0.0016$ and *$p = 0.0164$). F: Tumor area measurements in external controls size-matched to the NTAPP-treated tumors ($n = 31$) and to the internal controls ($n = 34$) from seven UV-exposed mice ($p = 0.0823$ and $p = 0.0608$, respectively). Dotted lines within the violin plots indicate the quartiles, while the dashed line represents the median.

treatments delivered within one week.

In the NTAPP-treated group, the treatment sites showed signs of considerable inflammation and crusting, and the majority of the tumors disappeared. While in the internal control tumor group, only a small percent of the untreated tumors disappeared spontaneously. In the external control group, the disappearance rate was similar to the internal controls, with 2/31 and 6/34 of tumors spontaneously involuting during the observation period, indicating that an abscopal effect was unlikely to be the reason for tumor disappearance in the internal controls. The size-matched external control tumors from the untreated mice showed an increase in the area similar to the internal control tumors. However, the increase in the size-matched tumors was not statistically significant. The differences between the tumor thicknesses measured with OG-HFUS before and after NTAPP showed a significant reduction in thickness by the 28-day follow-up, while internal control tumors in the treated mice increased in size. However, the latter increase was not statistically significant. In contrast, the thickness of external control tumors remained unchanged. Thus, the HFUS assessment of the treated sites provided further evidence of the efficacy of NTAPP.

Our findings on the efficacy of NTAPP in tumor treatment align with the limited prior data in the literature about the effectiveness of NTAPP in treating cutaneous tumors. Specifically, Kang et al. showed that NTAPP for 20 days in sixteen mice efficiently decreased the size of subcutaneous tumors formed by FaDu head and neck cancer cell lines [42]. Meanwhile, plasma treatment was cytotoxic and reduced the metabolic activity of SCC cell lines in vitro [23]. Additionally, cold atmospheric plasma potentially sensitizes head and neck cancers to chemotherapy and immune checkpoint blockade therapy [43], and

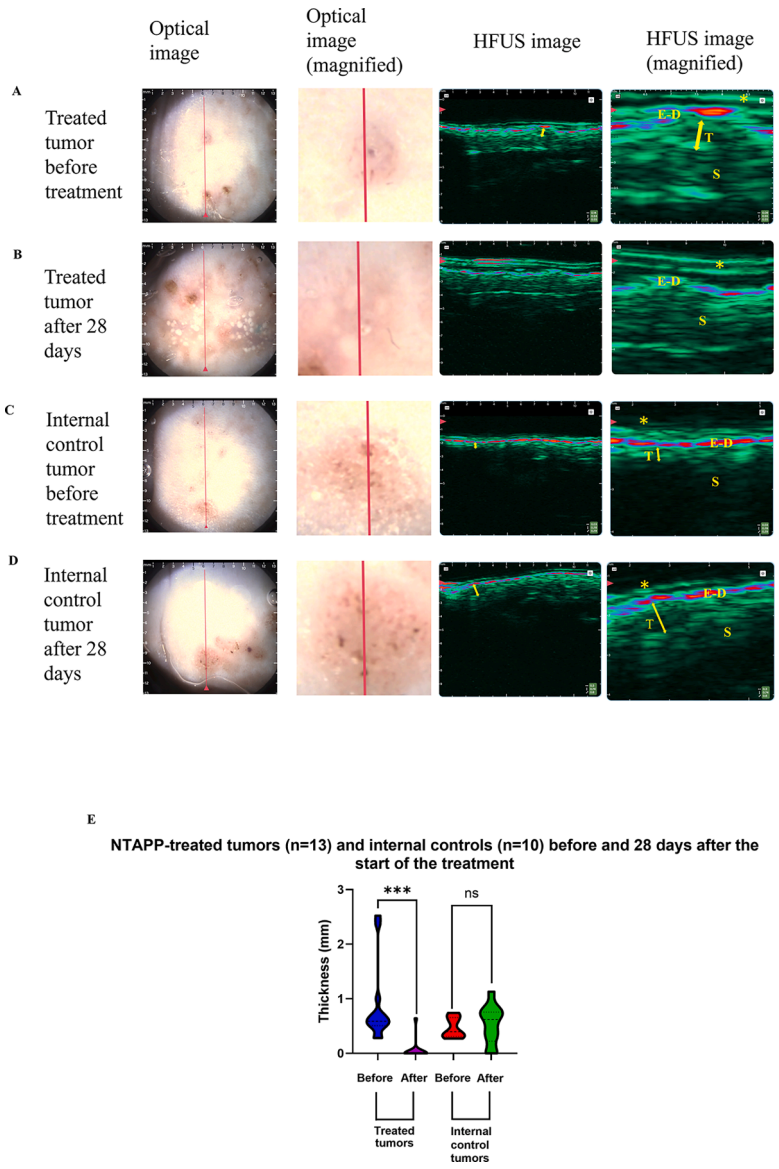


Fig. 2. Treatment Effects on Tumor Thickness After NTAPP Treatment. Optically guided high-frequency ultrasound (OG-HFUS) images of a representative NTAPP treated ($n = 13$) and internal control tumors ($n = 10$) before treatment and at 28 days follow-up. Dermoscopy and HFUS images of representative NTAPP-treated tumor before treatment (A) and the residual scar at the NTAPP treatment site (B) at the 28-day follow-up. Non-treated internal control tumor before treatment (C) and at the 28-day follow-up (D). The first column shows 13 mm × 13 mm optical dermoscopy images, and the second column shows 4.33x magnified optical images of the areas of interest, 3 mm × 3 mm. The third columns show the 12 mm × 12 mm HFUS images, and the fourth column has 4x magnified HFUS images corresponding to a 3 mm × 3 mm area. The red line on the optically guided images shows the surface of the skin where the HFUS image was captured. In the magnified images, yellow E-D: epidermis and dermis, S: subcutis T: tumor, *: ultrasound membrane. The yellow double-headed arrows mark the tumor thickness measurement. Mean NTAPP treated and internal control tumors (E) tumor thickness. ***: $p < 0.001$, ns: non-significant. Treated tumors ($n = 13$) showed a significant decrease in thickness 28 days after the beginning of the treatment (***$p = 0.0006$) compared to the internal control tumors ($n = 10$), which became thicker with time (ns, $p = 0.55$). Dotted lines within the violin plots indicate the quartiles, while the dashed line represents the median.

could be used as a potential adjuvant therapy [44]. Furthermore, NTAPP and cisplatin together had a synergic effect on skin cancer cells in vitro [45]. These prior findings, together with our studies, suggest the remarkable response of skin tumors to NTAPP and that it is reasonable to test NTAPP in neoadjuvant or combination treatments. Additional studies can elucidate the cellular mechanisms responsible for tumor involution and the of specific signaling pathways, cell proliferation and apoptosis in NTAPP response. Investigating the effect of NTAPP on tumors at varying stages of progression, could also provide valuable insights into the potential use of NTAPP in human therapeutic settings.

Most prior research on the effect of NTAPP in skin cancer treatment has been carried out in vitro and in vivo using subcutaneously implanted fast-growing tumors with limited ability to translate into the clinical setting. Our experiments were performed in a UV-induced skin tumor SKH1 mouse model to address these limitations. Although this model approximates human cutaneous carcinogenesis better than previously used models, it still has limitations. Differences between SKH1 mouse and human skin are apparent and may result in differences when our work is translated into human clinical studies. SKH1 mouse skin is thinner [46] and has less pigment [47], and this mouse lacks hair, but not hair follicles (or the remnant of hair follicles, so-called utriculi [48]), and hair follicles are denser, compared to human skin [49]. Therefore, treatment doses for mouse skin may differ from those for human skin. Nevertheless, findings of effective short-term NTAPP treatment in the SKH1 preclinical model are still expected to be applicable to human skin carcinogenesis.

Our study demonstrates the potential of NTAPP to effectively eliminate 74 % of UV-induced mouse tumors, an elimination rate in line with the response of early SCCs to photodynamic therapy in human skin [50]. Although, this response rate is inferior to the efficacy of surgical treatments it still suggests that NTAPP may present an excellent salvage treatment alternative especially if novel NTAPP protocols or combination treatment protocols with improved response rates are established.

The gold standard treatments for cSCC are surgical excision or Mohs micrographic surgery, which offer histological confirmation of the removal of the tumor and the highest cure rate for the most aggressive cSCC [51]. However, for in situ tumors, electrodesiccation and curettage are also frequently performed, while in unresectable locally advanced tumors, radiation treatment and systemic chemotherapy or immunotherapy are commonly offered [52–55]. In the management of invasive cSCC, when conventional treatment approaches are unsuitable or declined by the patient, salvage treatment options can be considered. The salvage treatment options currently usually include intralesional chemotherapy, cryotherapy, and photodynamic therapy (PDT). Intralesional 5-fluorouracil (5FU) and intralesional methotrexate (Methotrexate) chemotherapies are considered in patients with high disease burden for low-risk tumors, but despite their promise, they are seldom used as they require frequent clinic visits for numerous injections and the regulatory hurdles of handling chemotherapeutic medications [56, 57]. Of the salvage treatment options, only PDT and cryotherapy offer treatment in a single treatment setting [58], but both induce considerable discomfort. Based on the less-painful nature of NTAPP treatment [33,34] and the efficacy of NTAPP in inducing outstanding tumor resolution in a short treatment course, we provide crucial preclinical evidence that NTAPP may offer a promising salvage treatment option for low-risk cSCC and possibly other low-risk cutaneous malignancies.

CRediT authorship contribution statement

Szabolcs Bozsányi: Writing – review & editing, Writing – original draft, Visualization, Validation, Software, Resources, Project administration, Methodology, Investigation, Formal analysis, Data curation, Conceptualization. **Ruby Acquah:** Writing – review & editing, Validation, Investigation, Formal analysis, Data curation. **Rhea Carmel Glen Rodrigues:** Writing – review & editing, Validation, Investigation, Formal analysis, Data curation. **Erin C. Tracy:** Writing – review & editing, Validation, Supervision, Project administration, Methodology, Investigation, Conceptualization. **Sean P. Murphy:** Writing – review & editing, Methodology, Investigation, Conceptualization. **Gregory Fridman:** Writing – review & editing, Writing – original draft, Visualization, Supervision, Software, Resources, Methodology, Funding acquisition, Conceptualization. **Wendy J. Huss:** Writing – review & editing, Writing – original draft, Visualization, Validation, Supervision, Resources, Project administration, Methodology, Funding acquisition, Conceptualization. **Peter C. Friedman:** Writing – review & editing, Writing – original draft, Visualization, Validation, Supervision, Software, Funding acquisition, Conceptualization. **Gyorgy Paragh:** Writing – review & editing, Writing – original draft, Visualization, Validation, Supervision, Resources, Funding acquisition, Conceptualization.

Declaration of competing interest

The authors declare the following financial interests/personal relationships which may be considered as potential competing interests: Gyorgy Paragh reports a relationship with Sanofi-Aventis US LLC that includes: consulting or advisory. If there are other authors, they declare that they have no known competing financial interests or personal relationships that could have appeared to influence the work reported in this paper.

Acknowledgments

We express our gratitude to Dr. Gergely Csány and Dr. Miklós Gyöngy and their entire team at Dermus Ldt®, who provided exceptional technical and software support for the HFUS component for the work. We express our gratitude to Dr. Sydney Grant for her guidance and help with the materials. We express our gratitude to Dr. Deanne Connors, Dr. Pamela A. Hershberger, and the Trainee Writing group for their help with the manuscript. We would like to express our sincere gratitude to Dr. Li Yan`s valuable assistance with the statistical analysis. This work was supported by funds from Roswell Park Comprehensive Cancer Center and the National Cancer Institute (NCI) grant P30CA016056.

Data availability

Data will be made available on request.

References

[1] L. Andreassi, UV exposure as a risk factor for skin cancer, Expert. Rev. Dermatol 6 (5) (2011) 445–454.
[2] C. Kennedy, R. Willemze, F.R. de Gruijl, J.N.B. Bavinck, C.D. Bajdik, The influence of painful sunburns and lifetime sun exposure on the risk of actinic keratoses, seborrheic warts, melanocytic nevi, atypical nevi, and skin cancer, J. Invest. Dermatol. 120 (6) (2003) 1087–1093.
[3] B.C. Vitasa, H.R. Taylor, P.T. Strickland, F.S. Rosenthal, S. West, H. Abbey, et al., Association of nonmelanoma skin cancer and actinic keratosis with cumulative solar ultraviolet exposure in Maryland watermen, Cancer 65 (12) (1990) 2811–2817.
[4] L.L. Griffin, F.R. Ali, J.T. Lear, Non-melanoma skin cancer, Clin. Med. 16 (1) (2016) 62.
[5] G.P. Pfeifer, Mechanisms of UV-induced mutations and skin cancer, Genome Instab. Disease 1 (3) (2020) 99–113.
[6] A. Combalia, C. Carrera, Squamous cell carcinoma: an update on diagnosis and treatment, Dermatol. .Pract Concept 10 (3) (2020).
[7] F. Benavides, T.M. Oberyszyn, A.M. VanBuskirk, V.E. Reeve, D.F. Kusewitt, The hairless mouse in skin research, J. Dermatol. Sci. 53 (1) (2009) 10–18.
[8] S.J. Cooper, J. MacGowan, J. Ranger-Moore, M.R. Young, N.H. Colburn, G. T. Bowden, Expression of dominant negative c-jun inhibits ultraviolet B-induced squamous cell carcinoma number and size in an SKH-1 hairless mouse model, Mol. Cancer Res. 1 (11) (2003) 848–854.
[9] H.N. Ananthaswamy, A. Fourtanier, R.L. Evans, S. Tison, C. Medaisko, S.E. Ullrich, et al., p53 mutations in hairless SKH-hr1 mouse skin tumors induced by a solar simulator, Photochem. Photobiol. 67 (2) (1998) 227–232.
[10] E.A. Thompson, S. Zhu, J.R. Hall, J.S. House, R. Ranjan, J.A. Burr, et al., C/EBPα expression is downregulated in human nonmelanoma skin cancers and inactivation of C/EBPα confers susceptibility to UVB-induced skin squamous cell carcinomas, J. Invest. Dermatol. 131 (6) (2011) 1339–1346.
[11] M. Wirtz, I. Stoffels, J. Dissemond, D. Schadendorf, A. Roesch, Actinic keratoses treated with cold atmospheric plasma, J. Eur. Acad. Dermatol. Venereol. 32 (1) (2018) e37–ee9.
[12] L. Gan, S. Zhang, D. Poorun, D. Liu, X. Lu, M. He, et al., Medical applications of nonthermal atmospheric pressure plasma in dermatology, JDDG: J. der Deutschen Dermatologischen Gesellschaft 16 (1) (2018) 7–13.
[13] M. Keidar, D. Yan, J.H. Sherman, Plasma as a fourth state of matter, This content has been downloaded from IOPscience Please scroll down to see the full text (2019).
[14] F. Tan, Y. Wang, S. Zhang, R. Shui, J. Chen, Plasma dermatology: skin therapy using cold atmospheric plasma, Front. Oncol. 12 (2022) 918484.
[15] B. Haertel, T. Von Woedtke, K.-D. Weltmann, U. Lindequist, Non-thermal atmospheric-pressure plasma possible application in wound healing, Biomol. Ther. (Seoul) 22 (6) (2014) 477.
[16] S. Bekeschus, A. Schmidt, K.-D. Weltmann, T. von Woedtke, The plasma jet kINPen–A powerful tool for wound healing, Clin. Plasma. Med 4 (1) (2016) 19–28.
[17] J.-H. Hwang, H.-Y. Lee, K.B. Chung, H.J. Lee, J. Kim, K. Song, et al., Non-thermal atmospheric pressure plasma activates Wnt/β-catenin signaling in dermal papilla cells, Sci. Rep. 11 (1) (2021) 16125.
[18] J.W. Choi, S.U. Kang, Y.E. Kim, J.K. Park, S.S. Yang, Y.S. Kim, et al., Novel Therapeutic Effects of Non-thermal atmospheric pressure plasma for Muscle Regeneration and Differentiation, Sci. Rep. 6 (1) (2016) 28829.
[19] J. Park, H. Lee, H.J. Lee, G.C. Kim, D.Y. Kim, S. Han, et al., Non-thermal atmospheric pressure plasma efficiently promotes the proliferation of adipose tissue-derived stem cells by activating NO-response pathways, Sci. Rep. 6 (1) (2016) 39298.
[20] J. Park, H. Lee, H.J. Lee, G.C. Kim, S.-S. Kim, S. Han, et al., Non-thermal atmospheric pressure plasma is an excellent tool to activate proliferation in various mesoderm-derived human adult stem cells, Free Radical. Biol. Med. 134 (2019) 374–384.

[21] M.Y. Alkawareek, S.P. Gorman, W.G. Graham, B.F Gilmore, Potential cellular targets and antibacterial efficacy of atmospheric pressure non-thermal plasma, Int. J. Antimicrob. Agents 43 (2) (2014) 154–160.
[22] B. Kusakci-Seker, M. Demirayak-Akdemir, The effect of non-thermal atmospheric pressure plasma application on wound healing after gingivectomy, Int. Wound. J 17 (5) (2020) 1376–1383.
[23] G. Pasqual-Melo, T. Nascimento, L.J. Sanches, F.P. Blegniski, J.K. Bianchi, S. K. Sagwal, et al., Plasma treatment limits cutaneous squamous cell carcinoma development in vitro and in vivo, Cancers (Basel) 12 (7) (2020) 1993.
[24] J.W. Chang, S.U. Kang, Y.S. Shin, K.I. Kim, S.J. Seo, S.S. Yang, et al., Non-thermal atmospheric pressure plasma induces apoptosis in oral cavity squamous cell carcinoma: involvement of DNA-damage-triggering sub-G1 arrest via the ATM/p53 pathway, Arch. Biochem. Biophys. 545 (2014) 133–140.
[25] T. Von Woedtke, S. Reuter, K. Masur, K.-D. Weltmann, Plasmas for medicine, Phys. Rep. 530 (4) (2013) 291–320.
[26] D. Yan, J.H. Sherman, M. Keidar, Cold atmospheric plasma, a novel promising anti-cancer treatment modality, Oncotarget 8 (9) (2017) 15977.
[27] H.-R. Metelmann, D.S. Nedrelow, C. Seebauer, M. Schuster, T. von Woedtke, K.-D. Weltmann, et al., Head and neck cancer treatment and physical plasma, Clin. Plasma. Med 3 (1) (2015) 17–23.
[28] H.-R. Metelmann, C. Seebauer, V. Miller, A. Fridman, G. Bauer, D.B. Graves, et al., Clinical experience with cold plasma in the treatment of locally advanced head and neck cancer, Clin. Plasma. Med. 9 (2018) 6–13.
[29] P.C. Friedman, V. Miller, G. Fridman, A. Lin, A. Fridman, Successful treatment of actinic keratoses using nonthermal atmospheric pressure plasma: a case series, J. Am. Acad. Dermatol. 76 (2) (2017) 349–350.
[30] M. Keidar, R. Walk, A. Shashurin, P. Srinivasan, A. Sandler, S. Dasgupta, et al., Cold plasma selectivity and the possibility of a paradigm shift in cancer therapy, Br. J. Cancer 105 (9) (2011) 1295–1301.
[31] F. Utsumi, H. Kajiyama, K. Nakamura, H. Tanaka, M. Mizuno, S. Toyokuni, et al., Variable susceptibility of ovarian cancer cells to non-thermal plasma-activated medium, Oncol. Rep. 35 (6) (2016) 3169–3177.
[32] M. Keidar, A. Shashurin, O. Volotskova, M. Ann Stepp, P. Srinivasan, A. Sandler, et al., Cold atmospheric plasma in cancer therapy, Phys. Plasmas 20 (5) (2013).
[33] N.G.I. Mancera, R. López-Callejas, R. Peña-Eguiluz, B.G. Rodríguez-Méndez, A. Mercado-Cabrera, V.H.T. Rizo, et al., Wound healing after biopsy in the mobile oral mucosa using a nonthermal atmospheric pressure plasma, IEEE Trans. Radiat. Plasma Med. Sci. 6 (8) (2022) 928–935.
[34] N. Abdulsamee, Expanded tentacles of cold plasma energy in dentistry–review, EC Dent. Sci 11 (2017) 223–239.
[35] P.R. Cohen, Topical application of 5-fluorouracil 5 percent cream associated with severe neutropenia: discussion of a case and review of systemic reactions after topical treatment with 5-fluorouracil, Dermatol. Online J. 24 (4) (2018).
[36] L. Nerurkar, A. McColl, G. Graham, J. Cavanagh, The systemic response to topical aldara treatment is mediated through direct TLR7 stimulation as imiquimod enters the circulation, Sci. Rep. 7 (1) (2017) 16570.
[37] M.-L. Bafounta, A. Beauchet, P. Aegerter, P. Saiag, Is dermoscopy (epiluminescence microscopy) useful for the diagnosis of melanoma?: results of a meta-analysis using techniques adapted to the evaluation of diagnostic tests, Arch. Dermatol. 137 (10) (2001) 1343–1350.
[38] M.D. Abràmoff, P.J. Magalhães, S.J. Ram, Image processing with ImageJ, Biophot. Int. 11 (7) (2004) 36–42.
[39] S. Bozsányi, M. Boostani, K. Farkas, P. Hamilton-Meikle, N.N. Varga, B. Szabó, et al., Optically guided high-frequency ultrasound to differentiate high-risk basal cell carcinoma subtypes: a single-centre prospective study, J. Clin. Med. 12 (21) (2023) 6910.
[40] N.N. Varga, M. Boostani, K. Farkas, A. Bánvölgyi, K. Lőrincz, M. Posta, et al., Optically guided high-frequency ultrasound shows superior efficacy for preoperative estimation of breslow thickness in comparison with multispectral imaging: a single-center prospective validation study, Cancers (Basel) 16 (1) (2023) 157.
[41] C. Welz, S. Emmert, M. Canis, S. Becker, P. Baumeister, T. Shimizu, et al., Cold atmospheric plasma: a promising complementary therapy for squamous head and neck cancer, PLoS One 10 (11) (2015) e0141827.
[42] S. Kang, J. Cho, J. Chang, Y. Shin, K. Kim, J. Park, et al., Nonthermal plasma induces head and neck cancer cell death: the potential involvement of mitogen-activated protein kinase-dependent mitochondrial reactive oxygen species, Cell. Death. Dis. 5 (2) (2014) e1056. -e.
[43] Y. Wang, X. Mang, D. Li, Z. Wang, Y. Chen, Z. Cai, et al., Cold atmospheric plasma sensitizes head and neck cancer to chemotherapy and immune checkpoint blockade therapy, Redox. Biol. (2023) 102991.
[44] X. Li, X. Rui, D. Li, Y. Wang, F. Tan, Plasma oncology: adjuvant therapy for head and neck cancer using cold atmospheric plasma, Front. Oncol. 12 (2022) 994172.
[45] C.-M. Lee, Y.-I. Jeong, M.-S. Kook, B.-H. Kim, Combinatorial effect of cold atmosphere plasma (Cap) and the anticancer drug cisplatin on oral squamous cell cancer therapy, Int. J. Mol. Sci. 21 (20) (2020) 7646.
[46] N.V. Gopee, D.W. Roberts, P. Webb, C.R. Cozart, P.H. Siitonen, J.R. Latendresse, et al., Quantitative determination of skin penetration of PEG-coated CdSe quantum dots in dermabraded but not intact SKH-1 hairless mouse skin, Toxicol. Sci. 111 (1) (2009) 37–48.
[47] R.L. Konger, E. Derr-Yellin, D. Hojati, C. Lutz, J.P. Sundberg, Comparison of the acute ultraviolet photoresponse in congenic albino hairless C57 BL/6J mice relative to outbred SKH 1 hairless mice, Exp. Dermatol. 25 (9) (2016) 688–693.
[48] U.H. Olesen, K. Jacobsen, C.M. Lerche, M. Haedersdal, Repeated exposure to fractional CO2 laser delays squamous cell carcinoma formation and prevents clinical and subclinical photodamage visualized by line-field confocal optical coherence tomography and histology, Lasers Surg. Med. 55 (1) (2023) 73–81.
[49] J.P. Sundberg, L.E. King Jr, R.V Kuiper, Skin, hair, and nails, Pathol. Genet. Eng. Other Mutant Mice (2021) 159–212.
[50] L. Lansbury, F. Bath-Hextall, W. Perkins, W. Stanton, J. Leonardi-Bee, Interventions for non-metastatic squamous cell carcinoma of the skin: systematic review and pooled analysis of observational studies, BMJ 347 (2013) f6153.
[51] D. Belkin, J.A. Carucci, Mohs surgery for squamous cell carcinoma, Dermatol. Clin. 29 (2) (2011) 161–174.
[52] D.E. Rowe, R.J. Carroll, C.L. Day Jr, Prognostic factors for local recurrence, metastasis, and survival rates in squamous cell carcinoma of the skin, ear, and lip: implications for treatment modality selection, J. Am. Acad. Dermatol. 26 (6) (1992) 976–990.
[53] R.M. Samstein, A.L. Ho, N.Y. Lee, C.A. Barker, Locally advanced and unresectable cutaneous squamous cell carcinoma: outcomes of concurrent cetuximab and radiotherapy, J. Skin Cancer 2014 (2014).
[54] R. Behshad, J. Garcia-Zuazaga, J. Bordeaux, Systemic treatment of locally advanced nonmetastatic cutaneous squamous cell carcinoma: a review of the literature, Br. J. Dermatol. 165 (6) (2011) 1169–1177.
[55] D. Ogata, T. Tsuchida, Systemic immunotherapy for advanced cutaneous squamous cell carcinoma, Curr. Treat. Options Oncol. 20 (2019) 1–9.
[56] K. Chitwood, J. Etzkorn, G. Cohen, Topical and intralesional treatment of nonmelanoma skin cancer: efficacy and cost comparisons, Dermatol. Surg. 39 (9) (2013) 1306–1316.
[57] L.M. Good, M.D. Miller, W.A. High, Intralesional agents in the management of cutaneous malignancy: a review, J. Am. Acad. Dermatol. 64 (2) (2011) 413–422.
[58] P.S. Fagerberg, I.M. Ramberg, P.B. Toft, Combining brachytherapy and cryotherapy as adjuvant therapy for squamous cell carcinoma of the conjunctiva: literature review and case reports, Ocul Oncol Pathol 7 (2) (2021) 77–84.